

Journal of Materials Chemistry B

Accepted Manuscript



This is an *Accepted Manuscript*, which has been through the Royal Society of Chemistry peer review process and has been accepted for publication.

Accepted Manuscripts are published online shortly after acceptance, before technical editing, formatting and proof reading. Using this free service, authors can make their results available to the community, in citable form, before we publish the edited article. We will replace this *Accepted Manuscript* with the edited and formatted *Advance Article* as soon as it is available.

You can find more information about *Accepted Manuscripts* in the [Information for Authors](#).

Please note that technical editing may introduce minor changes to the text and/or graphics, which may alter content. The journal's standard [Terms & Conditions](#) and the [Ethical guidelines](#) still apply. In no event shall the Royal Society of Chemistry be held responsible for any errors or omissions in this *Accepted Manuscript* or any consequences arising from the use of any information it contains.

ARTICLE

Stimulatory effects of the fast setting and suitable degrading Ca–Si–Mg cement on both cementogenesis and angiogenesis differentiation of human periodontal ligament cells

Cite this: DOI: 10.1039/x0xx00000x

Received 00th January 2012,
Accepted 00th January 2012

DOI: 10.1039/x0xx00000x

www.rsc.org/

Yi-Wen Chen^{a†}, Chia-Hung Yeh^{a†}, Ming-You Shie^{a*}

The purpose of this study is to develop a fast setting and suitable degrading Mg-calcium silicate cement (Mg-CS) and a mechanism using Mg ions to stimulate human periodontal ligament cells (hPDLs). Mechanical strength and stability has been determined by testing the diametral tensile strength; the degradation of the cements has been measured ascertaining the number of ions released in simulated body fluid. Other cell characteristics, such as proliferation, differentiation and mineralization, and hPDLs when cultured on cement surfaces, were also examined. The results show that the degradation rate of Mg-CS cements depends on the Mg content in CS. Regarding in vitro bioactivity, the CS cements were covered with clusters of apatite spherulites after immersion for 30 days, while there was less formation of apatite spherulites on the Mg-rich cement surfaces. In addition, the researchers also explored the effects of Mg ions on the cementogenesis and angiogenesis differentiation of hPDLs in comparison with pure CS cement. The proliferation, alkaline phosphatase, cementogenesis-related proteins (CEMP1 and CAP), and angiogenesis-related protein (vWF and ang-1) secretion of hPDLs were significantly stimulated when the Mg ion concentration of the medium was increased. The research results also suggest that Mg-CS cements with this modified composition stimulate hPDLs behaviour and so may be good biomaterials for bone substitutes and hard tissue regeneration applications as they stimulate cementogenesis/angiogenesis.

1 Introduction

Bone cements have been shown to have great potential for hard tissue regeneration by stimulating cell proliferation and forming calcified tissue.^{1–5} Among the variety of bone cements, calcium phosphate and calcium silicate have been most rigorously examined in regards to its benefits for bone formation.^{1,6–8} Although common β -tricalcium phosphate has been widely used as a bone defect substitute material due to its favorable biocompatibility, its biodegradation and osteostimulation properties are still far from optimal.^{9–12} In the recent years, calcium silicate-based (CS) cements have been developed as potential bioactive materials for use as bone substitute materials; some of them promote excellent in vitro and in vivo osteogenesis and odontogenesis.^{1–5} In our previous study, we produced a fast setting CS cement containing a combination of CaO, SiO₂, and Al₂O₃, which was shown to reduce setting time.^{1,6–8} In addition, CS cement not only exhibits good osteoconduction effects,^{9–12} but also reduces inflammation markers in primary human dental pulp cells (hDPCs).^{1,13} Previous reports show that CS based cements have the ability to promote osteogenesis differentiation of various stem cells, such as bone marrow stromal cells, adipose-derived stem cells, human dental pulp cells and periodontal ligament cells.^{1,14,15} The release of Si ion concentrations from CS

materials influences the behaviour of different cell types, such as inhibiting osteoclastogenesis in macrophage,⁷ and promoting angiogenesis in hDPCs.^{16,17} In addition, the amount of Si ions in CS-based materials can affect the adsorption of various extracellular matrices (ECM) such as collagen I, fibronectin, and vitronectin, and also promotes the up-regulation of MAPK/ERK and MAPK/p38, signalling the pathway more effectively than Ca components.¹

Other studies have found that the incorporation of metal ions into CS ceramics significantly enhances their bioactive properties, which has inspired us to consider the possibility that bioceramics with modified ions may be useful as an alternative approach to improving cell behaviour for tissue regeneration. In a previous study, Xia Li *et al.* synthesized mesoporous CaO–MO–SiO₂–P₂O₅ (M= Mg, Zn, Cu) bioactive glasses/composites to prove that the incorporation of Mg, Zn and Cu can easily tune hydroxyapatite crystallite size and morphology to provide wide application.¹⁸ In 2012, Jingxiong Lu *et al.* synthesized ordered mesoporous calcium–magnesium silicate (om-CMS) and reported that the om-CMS was degradable and had good bioactivity to facilitate cell proliferation, differentiation and attachment.¹⁹ Zhai *et al.* synthesized and analyzed the properties of Ca–Si–Mg-containing bioceramics, bredigite (Bre, Ca₇MgSi₄O₁₆), akermanite (Ake, Ca₂MgSi₂O₇) and diopside (Dio, CaMgSi₂O₆). These substances not only showed excellent

characteristics in vitro apatite precipitates, but also led to better mechanical properties than bioglass.^{20,21} In addition, Ca–Si–Mg bioceramics induce cell proliferation and osteogenic differentiation osteoblasts, and improve human mesenchymal stem cells and human adipose stem cells by up-regulation of bone-related genes expression of collagen I (COL I), alkaline phosphatase (ALP) and osteocalcin (OC).^{20,22} Due to the advantages of Ca–Si–Mg bioceramics for bone regeneration, it has been recommended that they be used for periodontal regeneration by stimulation of cementogenic/angiogenic differentiation of human periodontal ligament cells (hPDLs). Recently, several studies have investigated whether hPDLs constitutively express osteogenesis cytokines and growth factors, such as COL I, osteopontin, ALP, bone morphogenetic proteins, and anti-inflammatory cytokines.²³ Similarly, hPDLs are a potential candidate for periodontal tissue engineering and have been shown to differentiate osteoblastic, fibroblastic and cementoblastic lineages.²⁴ However, the mechanism through which Ca-Si-Mg stimulates cementogenic/angiogenic differentiation of hPDLs is not completely known. In this study, we investigate in vitro cementogenic/angiogenesis stimulation of Ca-Si-Mg cement for hPDLs as well as the possible mechanism underlying this process. Therefore, the interaction of both the Ca-Si-Mg cements and their ionic products with hPDLs is scientifically analyzed in this study, including cell proliferation, cementogenesis and angiogenesis differentiation of hPDLs. In addition, this study also investigates how the ions from three different Mg contents in CS cement affect the behaviour of hPDLs and the role of these ions in cementogenic and angiogenesis.

2 Materials and experiments

2.1 Preparation of specimens

The method used here for the preparation of CS powder has been described elsewhere.⁵ In brief, reagent grade SiO₂ (High Pure Chemicals, Saitama, Japan), CaO (Sigma-Aldrich, St. Louis, MO), and MgO (Sigma-Aldrich) powders were used as matrix materials (composition: 75% CaO + MgO, and 25% SiO₂). The nominal weight ratios of CaO–SiO₂–MgO are listed in Table 1. The oxide mixtures were then sintered at 1,400°C for 2 h using a high-temperature furnace and then ball-milled in ethyl alcohol using a centrifugal ball mill (S 100, Retsch, Hann, Germany) for 6 h. The sintered powder was mixed using a liquid/powder ratio of 0.35 mL/g. After being mixed with water, the cements were molded in a Teflod mold (diameter: 6 mm, height: 3 mm). There was enough cement to fully cover each well of the 24-well plate (GeneDireX, Las Vegas, NV) to a thickness of 2 mm for cell experiments. All samples were stored in an incubator at 100% relative humidity and 37°C for 1 day of hydration.

2.2 Setting time and strength

After the powder was mixed with liquid, the cements were placed into a cylindrical mould and stored in an incubator at 37°C and 100% relative humidity for hydration. The setting time of the cements was tested according to standards set by the International Standards Organization (ISO) 9917-1. For evaluation of the setting time, each material was analyzed using Gilmore needles (456.5 g), and the time was recorded when the needle failed to create a 1-mm deep indentation in three separate areas. After being taken out of the mould, the specimens were again incubated at 37°C in 100% humidity for

1 day. The diametral tensile strength (DTS) testing was conducted on an EZ-Test machine (Shimadzu, Kyoto, Japan) at a loading rate of 1 mm/min. The maximal compression load at failure was obtained from the recorded load-deflection curves. The ten specimens were examined for each of the materials.

2.3 Phase compositions and morphology

The phase composition of the cements was analyzed using X-ray diffractometry (XRD; Bruker D8 SSS, Karlsruhe, Germany), run at 30 kV and 30 mA at a scanning speed of 10/min. The morphology of the cement specimens were coated with gold and examined under a scanning electron microscope (SEM; JSM-6700F, JEOL) equipped with energy dispersive X-ray (EDX) operated in the lower secondary electron image (LEI) mode at 3 kV accelerating voltage.

2.4 Weight loss

The degree of degradation was determined by monitoring the weight change of the specimen following immersion in a simulated body fluid (SBF) solution. After drying at 60°C, the specimens were weighed both before and after immersion using a balance (TE214S, Sartorius, Goettingen, Germany). Ten specimens were examined for each of the materials investigated at each time point.

2.5 Cell isolation and culture

The hPDLs were freshly derived from caries-free, intact premolars that had been extracted from 3 healthy adults (18–24 years of age) for orthodontic treatment purposes. The patient gave informed consent, and approval from the Ethics Committee of the Chung Shan Medicine University Hospital was obtained (CSMUH No. CS14117). The teeth were instantly immersed into a phosphate-buffered saline (PBS; Caisson Laboratories, North Logan, UT, USA) containing 100 U/mL penicillin/streptomycin (Caisson) and kept immersed while they were transferred to the laboratory. The PDL tissues of the root surface were separated by blade, washed several times with PBS, and then cut into cubes. The tissue was broken down using 1 mL of 2 mg/mL type I collagenase (Sigma-Aldrich) and 4 mg/mL dispase (Sigma-Aldrich) for 30 min in the incubator. After the tissue fragments had been broken down, they were distributed into plates and cultured in DMEM, supplemented with 20% fetal bovine serum (FBS; Caisson), 1% penicillin (10,000 U/mL)/streptomycin (10,000 mg/mL) (PS, Caisson) and kept in a humidified atmosphere with 5% CO₂ at 37°C; the medium was changed every 3 days. The primary cells were then sub-cultured to obtain passage 0 single cell-derived clones (P0), and the passages P4–P6 were used for the following in vitro study. The cementogenic differentiation medium was DMEM supplemented with 10⁻⁸ M dexamethasone (Sigma-Aldrich), 0.05 g/L L-ascorbic acid (Sigma-Aldrich) and 2.16 g/L glycerol 2-phosphate disodium salt hydrate (Sigma-Aldrich). The angiogenic differentiation medium was DMEM supplemented with 2% fetal bovine serum, 1% penicillin/streptomycin, and 50 ng/mL vascular endothelial growth factor (Prospec, East Brunswick, NJ).

2.6 Cell morphology

After the cells had been seeded for 3 h, the specimens were washed three times with cold PBS and fixed in 1.5% glutaraldehyde (Sigma) for 2 h, after which they were dehydrated using a graded ethanol series for 20 min at each

concentration and dried with liquid CO₂ using a critical point dryer device (LADD 28000; LADD, Williston, VT). The dried specimens were then mounted on stubs, coated with gold, and viewed using Scanning electron microscopy (JEOL JSM-7401F, Tokyo, Japan).

2.7 Cell viability assays and ion concentration analysis

The hPDLs were suspended in a density of 10⁴ cells/ml and were directly seeded over each specimen at 37 °C in a 5% CO₂ atmosphere. After different culturing times, cell viability was evaluated using the PrestoBlue[®] assay (Invitrogen, Grand Island, NY). The reagent PrestoBlue[®] was used for real-time and repeated monitoring of cell cytotoxicity, which is determined based on the level of mitochondrial activity. To explain this process briefly, at the end of the culture period, the medium is discarded and the wells are washed twice with PBS. Each well is filled with a solution containing PrestoBlue[®] and fresh DMEM (1: 9) at 37°C for 30 min. The solution in each well is then transferred to a new 96-well plate. Plates are read using a multi-well spectrophotometer (Hitachi, Tokyo, Japan) at 570 nm with a reference wavelength of 600 nm. Cells cultured on a tissue culture plate are used as a control (Ctl). The results were obtained in triplicate from six separate experiments for each test.

The culture medium was quantitatively analyzed for Ca, Si, and Mg ions using an inductively coupled plasma-atomic emission spectrometer (ICP-AES; Perkin-Elmer OPT 1MA 3000DV, Shelton, CT, USA). Three samples were measured for each data point. The results were obtained in triplicate from three separate samples for each test.

2.8 Preparation of test medium containing different Mg concentration

One gram of cement was immersed in 10 mL of DMEM for 1 day and the supernatants were passed through a 0.22 µm filter (Millipore, Billerica, MA) to obtain a cement extract. The Ca, Si, and Mg ion concentrations of the extract were analyzed using an inductively coupled plasma-atomic emission spectrometer. A detailed description of the dilution of the test medium with various Mg ion concentrations is given elsewhere.⁷ The cement extract and DMEM were used to prepare three different media with various Mg ion concentrations (Table 2).

2.9 Cementogenic assay

The production of cementum protein 1 (CEMP1) and cementum attachment protein (CAP) released from cells were cultured on different specimens for 7 and 14 days were quantified using ELISA (Abcam). Following the manufacturer's procedure we used the assay, which has a higher sensitivity. The reaction was terminated by the addition of stop solution and read at 450 nm using a Tecan Infinite 200 Pro plate reader (Tecan, Männedorf, Switzerland). The concentrations of CEMP1 and CAP were determined from each standard curve of pure protein. Each experiment was performed three times.

were collected and quantified using the ELISA kit.

The protein concentration was measured by correlation with a standard curve. The analyzed blank disks were treated as controls. All experiments were done in triplicate.

2.10 Alizarin Red S stain

The accumulated calcium deposition was analyzed using Alizarin Red S staining, following a method developed for a previous study.²⁵ In brief, the specimens are fixed with 4% paraformaldehyde (Sigma-Aldrich) for 15 min and then incubated in 0.5% Alizarin Red S (Sigma-Aldrich) at pH of 4.0 for 15 min at room temperature. After this, the cells are washed with PBS and photographs are taken using an optical microscope (BH2-UMA, Olympus, Tokyo, Japan) equipped with a digital camera (Nikon, Tokyo, Japan) at 200x magnification. The Alizarin Red is also quantified using a solution of 20% methanol and 10% acetic acid in water. After 15 min, the liquid is transferred to a 96-well, and the quantity of Alizarin Red is determined using a spectrophotometer at 450 nm.

2.11 Angiogenic assay

The production of ang-1 and vWF were quantified using ELISA kits (Abcam, catalog no. ab99970 and ab108918) according to the manufacturer's instructions. To summarize this process briefly, the hPDLs are cultured on substrates for 3 and 7 days, and proteins from the whole cell lysates are then collected and quantified using the ELISA kit. In addition, the Matrigel in vitro angiogenesis assay is used (Corning, MA, USA) to evaluate the angiogenic properties of hPDLs cultured in different media. After being cultured for 1 day, the cells are photographed using an inverted microscope (Olympus, Tokyo, Japan).

2.12 The effects of Ca-Si-Mg extracts of hPDLs behaviour

To further investigate the differences in the effects of ionic extracts from those of cement on cell behavior, hPDLs were cultured in each concentration of extracts supplemented with 10% FBS and 1% P/S in the 96-well plates for 1, 3 and 7 days. The proliferation assay, as well as cementogenic and angiogenic assays, was performed as described in the previous section.

2.13 Statistical analysis

A one-way variance statistical analysis was used to evaluate the significance of the differences between the groups in each experiment. Scheffe's multiple comparison test was used to determine the significance of the deviations in the data for each specimen. In all cases, the results were considered statistically significant with a *p* value < 0.05.

3 Results and discussion

3.1. Setting time and strength of cements

The powder and liquid are mixed in an appropriate ratio to form a paste that hardens through the interaction of the crystals precipitated in the paste when it is at body temperature. Thus, the setting time is one of most important factors in the clinical use of this compound.²⁶ The long setting time will lead to clinical problems under certain conditions. We propose that 10–15 min is a suitable setting time interval in the clinical.²⁷ The setting time of all cement specimens used in this study are listed in Table 1. The setting time of the cements increase when the Mg content is increased; the setting time of the Mg, incorporated with different amounts of calcium silicate, can be ranged from 19 min (Mg0) to 33 min (Mg20). When the

concentration of Mg increased, the setting time of cements also increased. Because MgO and the decrease of Ca content in the cements led to the decreased formation rate of hydroxyapatite substituted the CaO, the setting time of the cements with higher Mg concentration increased. Xia Li *et al.* also reported that Mg can suppress the crystallization of hydroxyapatite.¹⁸ In the present study, the setting time of calcium-silicate based cements is proportional to the amount of calcium silicate hydrate (CSH).^{9,28} CSH is able to decrease the setting time of the calcium-based cement. Our results show that a setting time of approximately 20 min for injectable bone cements for use in vertebroplasty and kyphoplasty is possible.¹² The DTS values of the hardened cements are 3.2, 3.4, 3.7 and 3.2 MPa, with the values changing in response to increases in the Mg content (Table 1). ANOVA Result shows significant differences between the DTS values of the four cements. Mg10 has the highest DTS value (3.7 MPa) in the group. Thus, differences in the phase composition of the hydration products may play a crucial role in the mechanical properties of these cements.

Table 1 Nominal composition, liquid-to-powder ratio, initial setting time, final setting time, and diametral tensile strength of the Mg-CS cements. Values not sharing a common letter are

Code	Ca:Si:Mg	L/P ratio (mL/g)	Initial setting time (min)	Final setting time (min)	DTS (MPa)
Mg0	75:25:0	0.3	4 ± 0.3 ^a	19 ± 0.8 ^c	3.2 ± 0.26 ^f
Mg5	70:25:5	0.32	4 ± 0.4 ^a	20 ± 0.6 ^{c,d}	3.4 ± 0.41 ^{f,g}
Mg10	65:25:10	0.33	5 ± 0.6 ^{a,b}	22 ± 1.2 ^d	3.7 ± 0.32 ^g
Mg20	55:25:20	0.35	6 ± 0.5 ^b	33 ± 2.1 ^e	3.2 ± 0.28 ^f

significantly different at $p < 0.05$.

3.2. Phase composition of cements

Figure 1A shows the XRD patterns of the specimens after hydration for 1 day. Mg0 has an obvious diffraction peak near $2\theta = 29.4^\circ$, which corresponds to the CSH gel, and incompletely reacted inorganic component phases of the β -dicalcium silicate (β -Ca₂SiO₄) at 2θ between 32° and 34° .²⁸ Contrary to our findings, the appearance of a poorly crystalline CSH gel was the principal hydration product of Mg-rich specimens such as Mg10 and Mg20. The specimens containing Mg showed that the cements are mainly composed of bredigite phase (JCPDS 33-0399). The broad peak of the magnesium silicate hydrate (MSH) gel phase seems to overlap with the incipient presence of a crystalline bredigite phase between 32° and 37° .²⁹ In addition, it could be seen that the apatite peak appeared after soaking of Mg0 and Mg5 (Fig. 1B). Apatite also formed on Mg10 and Mg20, but the intensity of peaks was low.

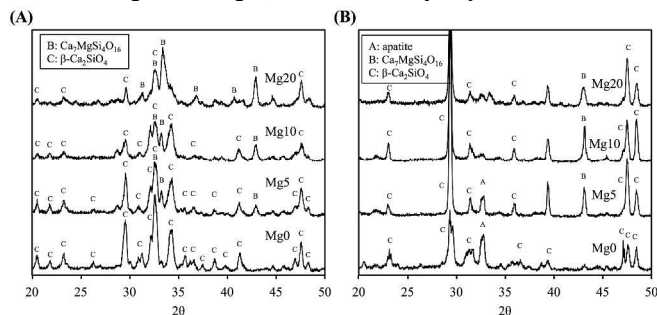


Fig. 1 XRD patterns of specimens (A) before and (B) after immersion in SBF at 37 °C for 1 day.

3.3. Characterization of immersed cements.

Bone mineral includes about 36.7% calcium, 16.0% phosphorus and various significant amounts of carbonate, sodium, potassium, magnesium, chloride, fluoride, and citrate ions. In bones and teeth, we can observe that Magnesium is always associated with the mineralization of calcified tissues.³⁰ Magnesium indirectly affects mineral metabolism by promoting alkaline phosphatase activity, and directly influences the pattern of mineral formation and the crystallization processes of mineral substances.^{31,32} In order to investigate the phenomena of apatite precipitation of Mg-CS cements, the SEM images were examined. The surface microstructure of the specimens before and after soaking in SBF for 7 and 30 days is shown in Fig 2. It is readily visible that Mg0 exhibits a dense and smooth surface containing interlocking particles. It could be seen that most of the bredigite particles had sintered, and some micropores were evident. After immersion in SBF for 7 days, the Mg0 cement specimens induced the precipitation of the formation of an apatite layer. The formation of the apatite precipitates in SBF has proven to be useful in predicting the bone-bonding ability of material *in vitro*.³ For Mg-content specimens, it is evident that spherical granules precipitated on the surface of specimens after immersion and the morphology reveal an early stage of apatite precipitation. The apatite-forming ability of the specimen seems to be dependent on the Ca–Si ratio of the cements. Ca/P ratios of the SBF-immersed specimens were 1.69, 1.76, 2.01, and 2.32 for Mg0, Mg5, Mg10, and Mg20, respectively, which significantly ($p < 0.05$) increased with increasing Mg content. The Si–OH functional groups on the surface of calcium silicate-based materials have been shown to act as nucleation centers for apatite precipitation.^{28,33} The release of Ca ions, possibly originating from the less-ordered hydration products, could significantly promote apatite growth by promoting local Ca supersaturation, as reported in a previous study,⁴ thereby raising the ionic product of the apatite in the surrounding environment and promoting the nucleation rate of the apatite.

After soaking for 30 days, Mg0 the surface appears to mainly be smooth, with intermingled particles. However, in the specimens containing Mg it appears that a dissolution of the surface has taken place. The surface morphology of the Mg10 and Mg20 specimens altered significantly in the presence of the etching-induced micropores on the apatite layer. Degradability plays an important role in biodegradation, and so must be considered when trying to develop a material that has a degradation rate most appropriate to hastening and easing the process of bone regeneration.² With this in mind, the degradation rates of the Mg-contained CS in SBF solution have been recorded for different time-points, as shown in Fig. 3A. When immersed in SBF, all specimens show a decrease in weight loss with the increase in soaking time, a decrease of 6–9% after 1 week. Mg10 and Mg20 both have more weight loss than Mg5 and Mg0. All the specimens exhibit an increased weight loss with an increase in the immersion time, reaching a maximum weight loss of 8–20% after 4 weeks, depending on the type of specimen. At the end of the immersion experiment (12 weeks), weight losses of 10.2%, 17.5%, 33.2%, and 41.5% were observed for Mg0, Mg5, Mg10, and Mg20, respectively, which indicates a significant difference ($p < 0.05$). In clinical use, it is known that bioactive materials with different degradation rates are required.³⁴ Kao *et al.* finds that the degradation rate of the calcium phosphate/calcium silicate composite cements increase with time when the calcium phosphate content is more than 20 wt%, and pure calcium silicate cement shows only a small amount of weight loss.²⁸ Our results show that Mg contents in CS-based materials play an important role in determining the degradability of cements, and the degradation of cements may be

controlled by the adjustment of Mg content. We suggested that the higher degradation rate of the CS with higher Mg concentration was caused by its large surface area and pore volume in comparison with the CS without or with lower Mg concentration.¹⁹ Moreover, the crystal structure of materials is also affected by the degradation and mechanical properties of the cements.³⁵ The fast degradation rate of Mg limits its applications, especially as a bone substitute.³⁶ Wu and Chang assert that bredigite has a higher weight loss than akermanite and diopside after being soaked in SBF for 28 days.³⁷

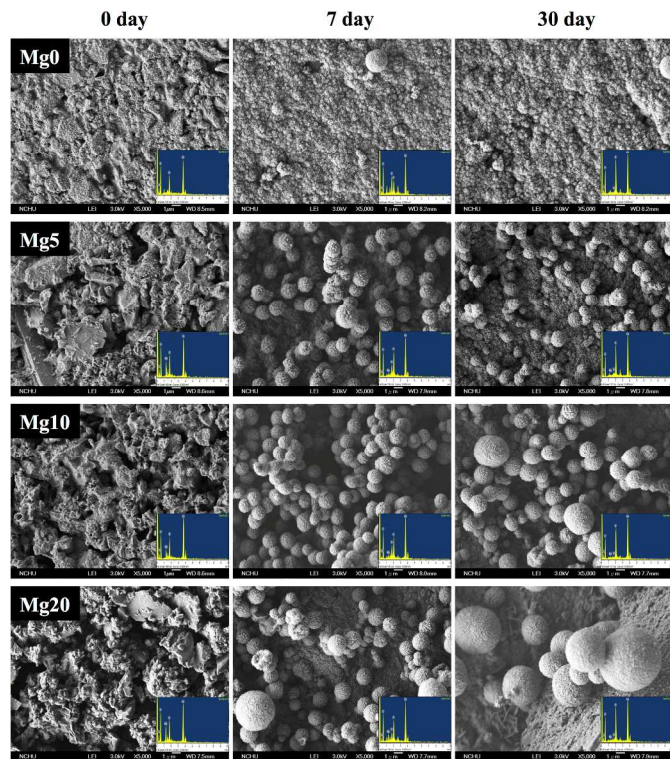


Fig. 2 SEM micrographs and EDX of Mg-contained CS surfaces before and after immersion in SBF for 7 and 30 days.

The DTS values of the as-set cement specimens were 3.2, 3.4, 3.7 and 3.2 MPa for Mg0, Mg5, Mg10, and Mg20, respectively. In previous study, Ismael H. García-Páez *et al.* reported that the tricalcium phosphate ceramics that contained 5 and 10% $\text{CaMg}(\text{SiO}_3)_2$ had much higher strength and Weibull modulus values than that without additions.³⁸ In our result, we can also observe that the DTS values of Mg5 and Mg10 were higher than Mg0. Otherwise, Mg20 had lower DTS value and we suggested that it might be due to the large surface area and pore volume of Mg20. The values of Mg0 after 1-, 3-, and 4-weeks of immersion were 5.1, 4.8, and 4.4 MPa, respectively. It should be noted that the strength of Mg20 declines significantly from the prepared strength of 3.64 to 2.03 MPa after soaking for 12 weeks ($p < 0.05$), a reduction of approximately 44.2%. The Mg10 significantly ($p < 0.05$) lost 28.7% in tensile strength after 12 weeks of immersion. In contrast, Mg0 increased by about 17.1%, which is significantly different ($p < 0.05$) from its original strength. We suggested the reduction of the DTS values with increasing of time was caused by the degradation phenomena (Fig. 3A). Moreover, CS contains Mg is a typical silicate-based cement that has shown great potential for hard tissue repair applications. It has previously been demonstrated that diopside ceramics have excellent mechanical strength and the ability to induce in vitro apatite-formation in SBF.²¹

3.4. Attachment, proliferation, cementogenic/angiogenic differentiation of hPDLs on Mg-CS substrates

The PrestoBlue[®] assay was used to quantitatively analyze cell proliferation. Results confirm that cells can indeed attach and proliferate on different substrates (Fig. 4). It was found that hPDLs cultured on pure CS and Mg-CS have a rapid growth rate, which increases with culture time. This rate is significantly higher ($p < 0.05$) than that of Ctl. However, the hPDLs proliferation on pure CS and Mg-CS are approximately the same ($p > 0.05$) on day 1. Interestingly, Mg20 elicits a significant increase, 12% and 17% on days 3 and 7 of being cultured, respectively, in comparison with the CS cement (Mg0). Previous studies have shown that increased concentrations of Mg ions in cell culture media can adversely affect cell proliferation, and Mg ions act as a mitogenic factor to promote cellular proliferation in vitro.^{39,40} Therefore, if there is indeed an increase in Mg ion concentration in the medium, it is most likely due to the dissolution of increased Mg-rich amorphous content.

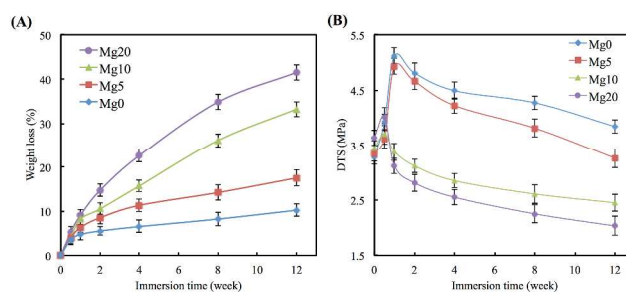


Fig. 3 (A) Weight loss and (B) diametral tensile strength of various cements after immersion in SBF for predetermined time durations.

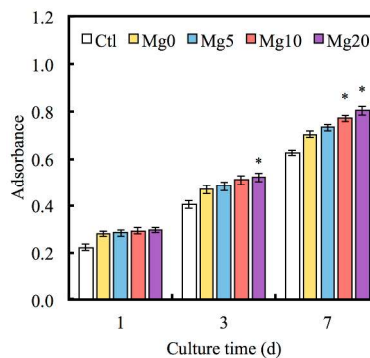


Fig. 4 The cell proliferation of hPDLs on different groups. “**” indicates a significant difference ($p < 0.05$) compared to Mg0.

Periodontal ligament cells have garnered considerable attention in periodontal tissue engineering research because of their great proliferation behavior and differentiation potential.⁴¹ Thus, it is of great importance to prepare suitable bioactive cements to promote the response of hPDLs for better periodontal tissue regeneration. The adhesion and proliferation of hPDLs on various Mg-CS specimens is shown in Fig 5. At hour 3, hPDLs adhered to the Mg10 and Mg20 surfaces were spread out, with round cells attaching to the Mg0 and Mg5 surfaces. After being cultured for 3 days, the SEM images reveal hPDLs spread and grow well on all specimens. Cells seem to colonize well on the specimens' surface, highlighting an evident adhesion and spreading, thus confirming previous reports of cell proliferation. In addition, the numbers of hPDLs adhering on the cements proliferated with the increase of

culture time, indicating good cytocompatibility of Mg-containing CS materials.⁴²

Table 2. The Ca, Si, Mg, and P concentration of the four ceramic extracts and test medium (means \pm SD, mM).

	Ca	Si	Mg	P
DMEM	1.74 \pm 0.03	0.00 \pm 0.00	0.95 \pm 0.04	0.95 \pm 0.04
Ca-free DMEM	0.00 \pm 0.00	0.00 \pm 0.00	0.94 \pm 0.04	0.95 \pm 0.04
Mg0	0.71 \pm 0.02	1.09 \pm 0.11	0.95 \pm 0.04	0.61 \pm 0.03
Mg5	0.74 \pm 0.04	1.48 \pm 0.16	1.83 \pm 0.05	0.72 \pm 0.06
Mg10	0.84 \pm 0.04	1.84 \pm 0.19	2.01 \pm 0.06	0.71 \pm 0.05
Mg20	0.90 \pm 0.03	2.11 \pm 0.16	2.97 \pm 0.07	0.77 \pm 0.06
Si0	0.51 \pm 0.03	0.00 \pm 0.00	0.98 \pm 0.03	0.85 \pm 0.03
M1	0.50 \pm 0.02	1.05 \pm 0.13	1.03 \pm 0.06	0.81 \pm 0.07
M1.5	0.45 \pm 0.04	1.05 \pm 0.11	1.48 \pm 0.05	0.79 \pm 0.08
M2	0.45 \pm 0.06	1.06 \pm 0.16	1.98 \pm 0.06	0.81 \pm 0.07

M1: Ca-free DMEM + Mg10 + Mg0 in a 2.5: 2.5: 5 volume ratios

M1.5: Ca-free DMEM + Mg10 in a 1: 1 volume ratio

M2: Ca-free DMEM + Mg20 in a 1: 1 volume ratio

CS-based materials have been shown to induce osteogenic and cementogenic differentiation in various cell types.¹⁶ To investigate the potential of the hPDLs for cementblast differentiation after being cultured on Mg-CS materials, the hPDLs were cultured for up to three days to evaluate the protein expression levels of differentiation markers using ELISA. In ALP, the Mg10 and Mg20 were markedly up regulated, which their differences significantly increased ($p < 0.05$) by 22% and 34%, respectively compared with Mg0 on day 3 (Fig. 7A). In cementogenic protein, the CEMP1 (Fig. 6B) and CAP (Fig. 6C) expression of hPDLs are also examined. Significant (25% and 35%) increases ($p < 0.05$) in the CEMP1 and CAP levels were found for Mg20 in comparison with the Mg0 after 14 days. In addition, to determine the effects of different substrates on mineralization in the hPDLs, we examined mineralized nodule formation in these cells using Alizarin Red S staining (Fig. 6D), as this can reveal details of bone nodule formation and calcium deposition. The results show that after 7 days Mg20 clearly increases the area of calcified nodules compared with Mg0. In previous studies we had shown that the viability of pulp cells and osteoblast-like cells on CS are higher than Ctl for all culture times.⁴³ Shie et al. found that soluble factors from calcium silicate substrates may be more important for proliferation and osteogenic differentiation in a growth medium.²⁵ The complexity of the bone supporting apparatus makes periodontal tissue regeneration a challenging field, as it involves the regeneration of cementum, a functionally oriented PDL tissue and an alveolar bone in the periodontal defect. It has been demonstrated that hPDLs can be differentiated into various types of cells.⁴⁴ In recent years, several studies have focused on the interaction of biomaterials and mesenchyme-derived cells and their ability to promote periodontal tissue regeneration.²⁴ ALP activity is also associated with hard tissue formation, and is produced in high levels during the hard tissue formation phase. The CEMP1 protein has been characterized as a novel, cementum-specific protein expressed by PDL subpopulations and cementoblasts.⁴⁵ CAP has been found as a collagen-like protein and serves as a marker for cementoblastic progenitors of the hPDLs. It was found that Mg10 and Mg20 materials promote cell attachment and the proliferation of hPDLs.

Interestingly, Mg-CS cement significantly increases relative cementogenic protein (CEMP1 and CAP) and calcium deposition of hPDLs compared to those on the CS cement.

The protein expression levels of vWF and Ang-1 in hPDLs cultured on various specimens were evaluated on days 7 and 14 (Fig. 7). The vWF expression in Mg5, Mg10, and Mg20 after 7 days was enhanced 1.05, 1.23, and 1.53 times, respectively, as compared to that of Mg0 (Fig. 7A). The Ang-1 results shown in Fig. 7B can be seen to be similar to vWF-1, both showing a dose-dependent up-regulation in the specimens with an increased Mg content ($p < 0.05$). vWF is the most important protein involved in coagulation and thrombus formation. Following synthesis, it is found in secretory granules called Weibel-Palade bodies and in blood vessels, and is released both constitutively and in a regulated manner.⁴⁶ Ang-1 is another family of growth factors that plays an important role in vascular development.⁴⁷ Our data shows that Mg10 and Mg 20 specimens have a higher potential to promote vWF and ang-1 expression than the pure CS cement (Mg0) during angiogenesis.

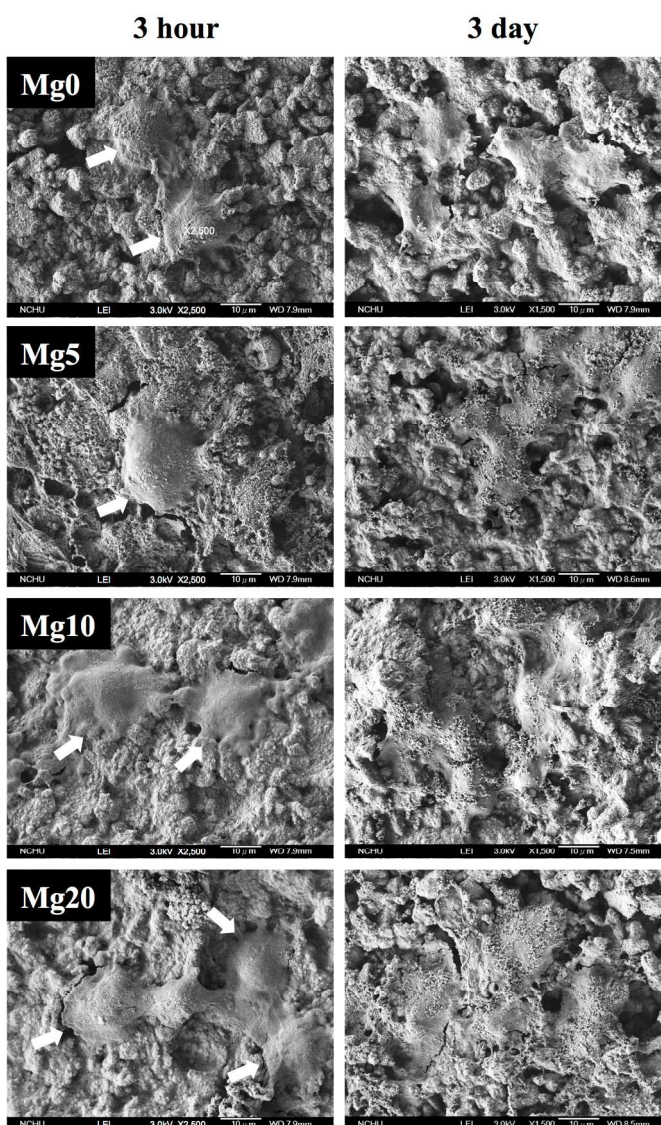


Fig. 5 SEM micrographs illustrating hPDLs morphologies on various specimens after different time-points of culture. At hour 3, the white arrows were indicated adhesion cells.

3.5. The effect of Mg concentration on hPDLs proliferation

Table 2 shows the Ca, Si, Mg, and P ion concentrations of the normal DMEM, Ca-free DMEM, Mg-CS extract, and the four prepared test media determined by ICP-AES. The P ion concentration found in normal and Ca-free DMEM was 0.95 mM, which is close to the original concentration (0.91 mM). The Ca concentration of normal DMEM was 1.74 mM, slightly different from the supplied concentrations of 1.80 mM. Both the Ca-free DMEM and normal DMEM lacked the Si component. In contrast, the Ca, Si, Mg, and P ion concentrations of the Mg20 extract were 0.90, 2.11, 2.97 and 0.77 mM, respectively. Ca, Si, and P ions concentrations of the test media conform to the required preparations that achieved a 0.5 mM increment in Mg at a fixed Ca, Si and P of around 0.5, 1.0, and 0.8 mM, respectively. In the present study, the results show that the Ca, Si, and Mg containing ionic products from the dissolution of Mg-CS materials at certain concentration ranges stimulate cell behavior, which is in accordance with other studies, and suggests that this stimulatory effect on cell proliferation and differentiation by ionic products can be considered as one criterion for the bioactivity of inorganic biomaterials.³⁷ Therefore, a medium with a constant 0.5 mM Ca and 1.0 mM Si was chosen to further evaluate the effects of various Mg ion concentrations on cell proliferation and consequent assays of cell function.

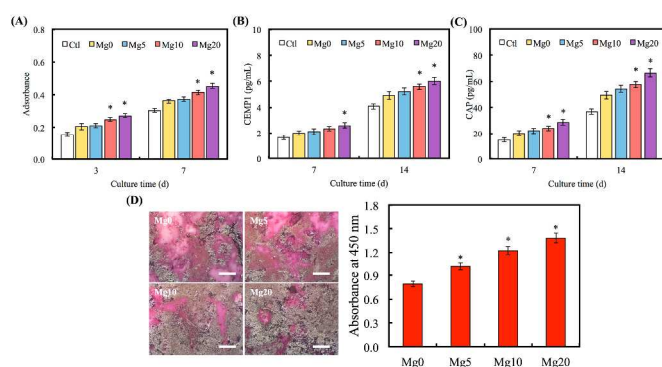


Fig. 6 (A) ALP activity, (B) CEMP1, and (C) CAP protein secretion from hPDLs were cultured on various substrates. “*”, statistically significant difference ($p < 0.05$) from CS. (D) Alizarin Red S staining of calcium mineral deposits by hPDLs cultured on Mg-CS for two weeks.

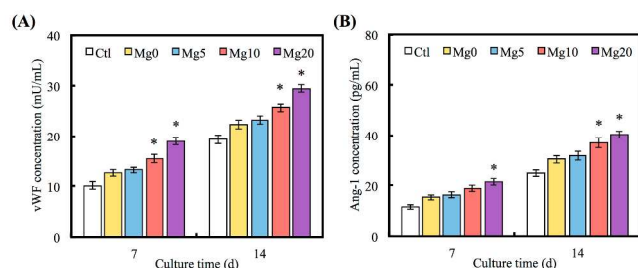


Fig. 7 (A) vWF and (B) ang-1 expression of hPDLs cultured on various specimens for different days. “*”, statistically significant difference ($p < 0.05$) from Mg0.

To investigate the effect of Mg ionic products from Mg-CS on proliferation of hPDLs, cells were cultured in cell culture plates with various mediums which were prepared from cement extract for 1, 3, and 7 days. The PrestoBlue[®] assay shows that the number of hPDLs cultured in all the mediums progressively

increased in proportion with increasing culture time, as shown in Fig. 8. Interestingly, more cells were found on M1 than on Si0 for all time-points ($p < 0.05$). In agreement with previous studies, the Si ion is a crucial factor in promoting primary cell activity.⁵ On day 3 the OD value of the hPDLs in the presence of M2 was 1.43, 1.19, and 1.13 times higher ($p < 0.05$) than those obtained in Si0, M1 and M1.5 medium, respectively. However, the proliferation rate of hPDLs on M1 and M1.5 were consistently similar ($p > 0.05$). Therefore, it may be suggested that Mg ions significantly promoted hPDLs proliferation. It is already well-established that Mg ions play an important role in stimulating cell proliferation, which can promote DNA and protein synthesis and regulate Mg conducting channels.⁴⁸ Otherwise, the cells cultured with Si0 medium showed the lowest OD value and this result pointed out the silicon is also an important component element of Mg-CS cement to facilitate cell proliferation. The previous reports showed that bone incorporates various nutrients in the form of trace elements and both Si and Mg have been found to play absolutely vital roles in the bone formation, growth, and regeneration and they are essential cofactors for enzymes which involve in the synthesis of the constituents of bone matrix.⁴⁹

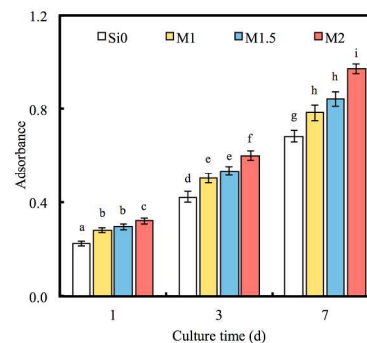


Fig. 8 Proliferation of hPDLs treated with medium contained different concentration of Si and Mg ions. Values not sharing a common letter are significantly different at $p < 0.05$.

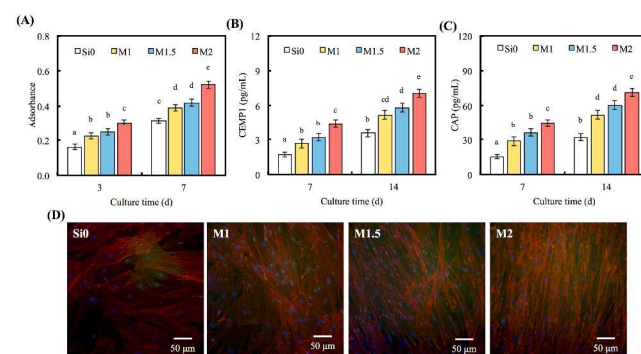


Fig. 9 (A) ALP activity, (B) CEMP1, and (C) CAP protein secretion from hPDLs were cultured with medium contained different concentration of Si and Mg ions. Values not sharing a common letter are significantly different at $p < 0.05$. (D) Immunofluorescence images of nuclei (blue), F-actin (red), and OC (green) in hPDLs cultured with different medium after 2 weeks.

3.6. The effect of Mg concentration on cementogenic/angiogenic differentiation of hPDLs

ALP activity of hPDLs in a medium containing different concentrations of Mg ions on days 3 and 7 was analyzed. As can be clearly seen in Fig. 9A, ALP activity in hPDLs with M2

is almost twice that of Si0, while there is no significantly difference between M1 and M1.5 (Fig. 9a). In addition, the results of CEMP1 (Fig 9B) and CAP (Fig 9C) show similar results, that is, M2 medium significantly enhances the cementogenic differentiation of hPDLs in comparison with other concentrations. We also further investigated the OC secretion by immunofluorescence microscopy after treatment in a different medium (Fig. 9D). Visual examination showed that hPDLs cultured with M1.5 and M2 have comparatively higher green fluorescence (OC) intensity than with Si0. Cells seeded on Matrigel formed an extensive lattice of vessel-like structures after 24 hours (Fig. 10A). The hPDLs cultured with M1.5 and M2 increased the size of the junctional area, and the thickness of the vessel-like structures increased. The vessel-like structures are significantly different than with Si0 and M1. ELISA analysis shows that the M1.5 and M2 medium significantly promotes vWF (Fig 10B) and ang-1 (Fig 10C) secretion in hPDLs, compared with Si0 and M1 ($p < 0.05$). However, Si0 and M1 showed no obvious difference ($p > 0.05$) at any of the time-points. Angiogenesis is critical for hard tissue regeneration, and angiogenic induction by bone substitutes itself is a simple and efficacious strategy for hard tissue regeneration.^{5,16} Angiogenesis during new bone formation has been examined in in vivo and in vitro experiments with calcium silicate-based materials.^{21,50} However, the mechanism by which Mg ions promotes cell activity, including initial cell proliferation and differentiation, remains unclear. In other words, it is unclear which factors from Mg contribute to its stimulation of cementogenesis and angiogenesis. Among them, M1.5 and M2 have higher Mg concentrations and greater stimulatory effects on angiogenesis induction than M1. These results imply a relationship between the induction of angiogenesis and Mg concentration.⁵¹

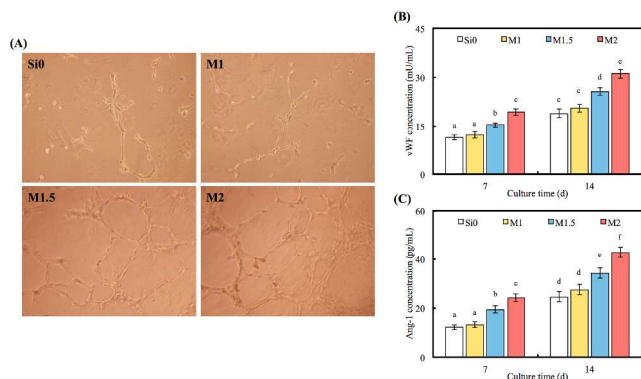


Fig. 10 (A) The tube formation, (B) vWF, and (C) ang-1 expression of hPDLs were treated with different medium. Values not sharing a common letter are significantly different at $p < 0.05$.

4 Conclusions

The results of the present study of newly developed Mg-calcium silicate cements shows that they are not only fast-setting and have good bioactivity, but also degrade in SBF. The ionic products of these materials' dissolution stimulate cell proliferation, cementogenic differentiation and angiogenesis. The degree of promotion varies depending on the Mg ion concentrations in the culture medium. In addition, Mg-CS also stimulates the proliferation of hPDLs in vitro and actively promotes the secretion of cementogenic (CEMP1 and CAP) and angiogenic (vWF and ang-1) proteins. The in vitro findings

provide the essential theoretical basis for further in vivo study of Mg-CS cements used as biomaterials in bone substitutes and bone regeneration applications.

Notes references

^a 3D printing Medical Research Center, China Medical University Hospital, Taichung City, Taiwan (E-mail: eviltacasi@gmail.com; +886-4-22052121; fax: +886-4-24759065).

† Y. W. Chen and C. H. Yeh are joint first authors.

Acknowledgements

The authors acknowledge receipt of a grant from China Medical University Hospital grants (DMR-104-103) and the Ministry of Science and Technology grants (MOST 104-2314-B-039-004) of Taiwan. The authors declare that they have no conflicts of interest.

References

- M. Y. Shie and S. J. Ding, *Biomaterials*, 2013, **34**, 6589–6606.
- S. H. Huang, Y. J. Chen, C. T. Kao, C. C. Lin, T. H. Huang, and M. Y. Shie, *J Dent Sci*, 2014.
- B. C. Wu, S. C. Youn, C. T. Kao, S. C. Huang, C. J. Hung, M. Y. Chou, T. H. Huang, and M. Y. Shie, *J Dent Sci*, 2014.
- C. H. Liu, T. H. Huang, C. J. Hung, W. Y. Lai, C. T. Kao, and M. Y. Shie, *Int Endod J*, 2014, **47**, 843–853.
- B. C. Wu, C. T. Kao, T. H. Huang, C. J. Hung, M. Y. Shie, and H. Y. Chung, *J Endod*, 2014, **40**, 1105–1111.
- C. T. Kao, M. Y. Shie, T. H. Huang, and S. J. Ding, *J Endod*, 2009, **35**, 239–242.
- C. J. Hung, C. T. Kao, Y. J. Chen, M. Y. Shie, and T. H. Huang, *J Endod*, 2013, **39**, 1557–1561.
- C. J. Hung, H. I. Hsu, C. C. Lin, T. H. Huang, B. C. Wu, C. T. Kao, and M. Y. Shie, *J Endod*, 2014, **40**, 1802–1809.
- C. C. Su, C. T. Kao, C. J. Hung, Y. J. Chen, T. H. Huang, and M. Y. Shie, *Mater Sci Eng C Mater Biol Appl*, 2014, **37**, 156–163.
- C. L. Chen, T. H. Huang, S. J. Ding, M. Y. Shie, and C. T. Kao, *J Endod*, 2009, **35**, 682–685.
- M. Y. Shie, D. C. H. Chen, C. Y. Wang, T. Y. Chiang, and S. J. Ding, *Acta Biomater*, 2008, **4**, 646–655.
- Y. F. Su, C. C. Lin, T. H. Huang, M. Y. Chou, J. J. Yang, and M. Y. Shie, *Mater Sci Eng C Mater Biol Appl*, 2014, **42**, 672–680.
- C. L. Chen, C. T. Kao, S. J. Ding, M. Y. Shie, and T. H. Huang, *J Endod*, 2010, **36**, 465–468.
- S. J. Ding, M. Y. Shie, T. Hoshiba, N. Kawazoe, G. Y. Chen, and H. C. Chang, *Tissue Eng Part A*, 2010, **16**, 2343–2354.
- S. C. Huang, B. C. Wu, C. T. Kao, T. H. Huang, C. J. Hung, and M. Y. Shie, *Int Endod J*, 2015, **48**, 236–245.
- T. T. Hsu, C. H. Yeh, C. T. Kao, Y. W. Chen, T. H. Huang, J. J. Yang, and M. Y. Shie, *J Endod*, 2015.
- M. Y. Chou, C. T. Kao, C. J. Hung, T. H. Huang, S. C. Huang, M. Y. Shie, and B. C. Wu, *J Endod*, 2014, **40**, 818–824.
- X. Li, X. Wang, D. He, and J. Shi, *J Mater Chem*, 2008, **18**, 4103–4109.
- J. Lu, J. Wei, Q. Gan, X. Lu, J. Hou, W. Song, Y. Yan, J. Ma, H. Guo, T. Xiao, and C. Liu, *Micropor Mesopor Mater*, 2012, **163**, 221–228.
- W. Zhai, H. Lu, C. Wu, L. Chen, X. Lin, K. Naoki, G. Chen, and J. Chang, *Acta Biomater*, 2013, **9**, 8004–8014.
- Y. Zhang, S. Li, and C. Wu, *J Biomed Mater Res Part A*, 2013, **102**, 105–116.
- H. Gu, F. Guo, X. Zhou, L. Gong, Y. Zhang, W. Zhai, L. Chen, L. Cen, S. Yin, J. Chang, and L. Cui, *Biomaterials*, 2011, **32**, 7023–7033.
- Y. J. Chen, M. Y. Shie, C. J. Hung, B. C. Wu, S. L. Liu, T. H. Huang, and C. T. Kao, *J Bone Miner Metab*, 2013, **32**, 671–682.
- X. Zhang, P. Han, A. Jaiprakash, C. Wu, and Y. Xiao, *J Mater Chem B*, 2014, **2**, 1415–1423.
- M. Y. Shie, S. J. Ding, and H. C. Chang, *Acta Biomater*, 2011, **7**,

- 2604–2614.
26. M. H. Huang, C. T. Kao, Y. W. Chen, T. T. Hsu, D. E. Shieh, T. H. Huang, and M. Y. Shie, *J Mater Sci: Mater Med*, 2015, **26**, 161.
 27. E. Fernández, F. J. Gil, M. P. Ginebra, F. C. M. Driessens, J. A. Planell, and S. M. Best, *J Mater Sci: Mater Med*, 1999, **10**, 223–230.
 28. C. T. Kao, T. H. Huang, Y. J. Chen, C. J. Hung, C. C. Lin, and M. Y. Shie, *Mater Sci Eng C Mater Biol Appl*, 2014, **43**, 126–134.
 29. T. Zhang, C. R. Cheeseman, and L. J. Vandeperre, *Cem Concr Res*, 2011, **41**, 439–442.
 30. H.-P. Wiesmann, T. Tkotz, U. Joos, K. Zierold, U. Stratmann, T. Szuwart, U. Plate, and H. J. Höhling, *J Bone Miner Res*, 1997, **12**, 380–383.
 31. A. Bigi, R. Gregorini, A. Ripamonti, N. Roveri, and J. S. Shah, *Calcif Tissue Inter*, 1992, **50**, 439–444.
 32. S. Tsuboi, H. Nakagaki, K. Ishiguro, K. Kondo, M. Mukai, C. Robinson, and J. A. Weatherell, *Calcif Tissue Inter*, 1994, **54**, 34–37.
 33. Y. Zhou, C. Wu, and Y. Xiao, *Acta Biomater*, 2012, **8**, 2307–2316.
 34. W. Liu, C. Wu, W. Liu, W. Zhai, and J. Chang, *J Biomed Mater Res Part B Appl Biomater*, 2013, **101**, 279–286.
 35. P. Ducheyne, S. Radin, and L. King, *J Biomed Mater Res Part A*, 1993, **27**, 25–34.
 36. M. Yazdimamaghani, M. Razavi, D. Vashae, and L. Tayebi, *Mater Sci Eng C Mater Biol Appl*, 2015, **49**, 436–444.
 37. C. Wu and J. Chang, *J Biomed Mater Res Part B Appl Biomater*, 2007, **83**, 153–160.
 38. I. H. García-Páez, R. G. Carrodeguas, A. H. De Aza, C. Baudin, and P. Pena, *J Mech Behav Biomed*, 2014, **30**, 1–15.
 39. S. S. Singh, A. Roy, B. E. Lee, I. Banerjee, and P. N. Kumta, *Mater Sci Eng C Mater Biol Appl*, 2014, **45**, 589–598.
 40. J. Fischer, M. H. Prosenc, M. Wolff, N. Hort, R. Willumeit, and F. Feyerabend, *Acta Biomater*, 2010, **6**, 1813–1823.
 41. A. Nanci and D. D. Bosshardt, *Periodontol. 2000*, 2006, **40**, 11–28.
 42. C. Wu, J. Chang, J. Wang, S. Ni, and W. Zhai, *Biomaterials*, 2005, **26**, 2925–2931.
 43. S. J. Ding, C. T. Kao, M. Y. Shie, C. C. Hung, and T. H. Huang, *J Endod*, 2008, **34**, 748–751.
 44. T. H. Huang, C. C. Chen, S. L. Liu, Y. C. Lu, and C. T. Kao, *Laser Phys Lett*, 2014, **11**, 075602.
 45. M. A. Alvarez-Perez, S. Narayanan, M. Zeichner-David, B. Rodríguez Carmona, and H. Arzate, *Bone*, 2006, **38**, 409–419.
 46. M. R. Williamson, R. Black, and C. Kielty, *Biomaterials*, 2006, **27**, 3608–3616.
 47. E. Mavrogonatou and D. Kletsas, *J Cell Physiol*, 2011, **227**, 1179–1187.
 48. E. Abed and R. Moreau, *Am J Physiol Cell Physiol*, 2009, **297**, C360–C368.
 49. R. Jugdaohsingh, L. D. Pedro, A. Watson, and J. J. Powell, *Bone Reports*, 2015, **1**, 9–15.
 50. M. Zhang, C. Wu, K. J. Lin, W. Fan, L. Chen, Y. Xiao, and J. Chang, *J Biomed Mater Res Part A*, 2012, **100**, 2979–2990.
 51. H. Li and J. Chang, *Acta Biomater*, 2013, **9**, 5379–5389.